Deviation from the Orbital Symmetry Rules. 1,2-Hydrogen Addition

Shogo Sakai

Department of Information Systems Engineering, Faculty of Engineering, Osaka Sangyo University, Daito 574, Japan

Received: June 25, 1996; In Final Form: October 30, 1996[⊗]

The reaction mechanisms of 1,2-hydrogen addition to the π bond of $H_2X{=}YH_2$ (X or Y = C, Si, B, N, Al, and P) type molecules were studied by ab initio molecular orbital methods. For reactions $H_2 + H_2C{=}CH_2$ and $H_2Si{=}SiH_2$, least-motion (C_{2v} symmetry) and reduced symmetry pathways (C_s or C_1 symmetries) were calculated. The reactions on these pathways were classified into two types (a *concerted* and a *polarized* mechanism) by the CI/LMO/CAS analysis. The reactions for both systems along the C_{2v} symmetry path belongs to the *concerted* mechanism (biradical type). On the C_s symmetry path, the reaction of ethylene also belongs to the *concerted* mechanism; the reaction of disilene belongs to the *polarized* mechanism. The energy barrier heights on the C_s (or C_1) symmetry pathway were reduced 17% for ethylene system and 22% for disilene system from those on the C_{2v} symmetry pathways by the MP2/CAS(6,6) method. The other reactions—X not equal to Y—were also classified into the *polarized* mechanisms by the CI/LMO/CAS analysis. The classification was explained on the basis of the triplet excitation and polarization energies of the π bond in $H_2X{=}YH_2$ model molecules.

I. Introduction

It is well-known that the orbital symmetry rules[1] are very useful for the decision of allowance and forbiddance of chemical reactions. One of the typical application examples of the rules is the addition of molecular hydrogen to ethylene via a four-center transition state, which is a prototypical reaction for molecule additions to unsaturated hydrocarbons.

$$H_2C{=}CH_2 + H_2 \rightarrow H_3C{-}CH_3 \qquad (1)$$

While the least-motion pathway with C_{2v} symmetry for reaction 1 is symmetry forbidden, the reduced symmetry (C_s or C_1) pathway is symmetry allowed from the precise treatment of the rules. The activation barrier heights on these reaction pathways could not be estimated from the rules. Gordon and co-workers[2] calculated the activation energy barrier height (130 kcal/mol) for 1,2-hydrogen elimination from ethane with reduced symmetry (C_s symmetry) by ab initio MO methods. The energy barrier (113.4 kcal/mol) for 1,2-hydrogen addition into ethylene with the C_s symmetry was also calculated by Siria and co-workers.[3] On the other hand, the reaction of $H_2Si{=}SiH_2 + H_2$ is also symmetry forbidden on the least-motion pathway and symmetry allowed on the reduced symmetry pathway. The potential energy surfaces for 1,2-hydrogen elimination processes for disilane were calculated by Gordon and co-workers.[4] They estimated the activation energy barrier of 86 kcal/mol on the reduced symmetry pathway by ab initio MO methods. However, the difference of energy barrier heights on the least-motion (C_{2v} symmetry) and the reduced symmetry pathways is, to our knowledge, unknown.

To clarify the influence of symmetry on the activation energy barriers for reactions, the reaction paths for 1,2-hydrogen addition to the π bond of seven $H_2X{=}YH_2$ molecules were studied in the view of symmetry and asymmetry (reduced symmetry).

II. Theoretical Approach

The basis set used here was the split-valence plus polarization 6-31G(d,p) set.[5] All equilibrium and transition state geometries were determined with analytically calculated energy gradients[6] at a complete active space (CAS) self-consistent-field (SCF) method[7] and the second-order Møller−Plesset perturbation (MP2) level[8] of theory with the Hartree−Fock wave functions using the 6-31G(d,p) basis set. For the CASSCF calculation, two types of active spaces were chosen. One is four active spaces corresponding to the π and π^* orbitals of $H_2X{=}YH_2$ and the σ and σ^* orbitals of the active hydrogen molecule (CAS(4,4)). The other is the active spaces of CAS(4,4) plus the σ and σ^* orbitals of X−Y bond (CAS(6,6)). For both of the CASSCF calculations, all configurations in the active spaces were generated. The force constant matrix and thereby the vibrational frequencies were calculated with analytically calculated energy second derivatives.[9] Additional calculations were performed to obtain improved energy comparisons—the calculations with the CASSCF-optimized structures with electron correlation incorporated through the multiconfigurational second-order Møller−Plesset perturbation theories [MP2/CAS][10] and the calculations with the MP2-optimized structures with electron correlation incorporated through the fourth-order Møller−Plesset perturbation theories [MP4(SDTQ)/MP2]. The intrinsic reaction coordinate[11] (IRC) was followed from the transition state toward both reactants and products.

To interpret reaction mechanisms along the reaction pathway, a configuration interaction (CI)/localized molecular orbital (LMO)/CAS analysis was carried out following a method described elsewhere[12,13] with the 6-31G(d,p) basis set. (1) The RHF, single-determinant wave function is calculated and the MOs that correspond most closely to the σ and σ^* orbitals of the active hydrogen part and the π and π^* orbitals of the $H_2X{=}YH_2$ part are identified. A four-orbital, four-electron CASSCF calculation (CAS(4,4)) is then performed to obtain a starting set of orbitals for the localization procedure. (2) After carrying out the CASSCF procedure, the CASSCF-optimized orbitals are localized. The four CASSCF-optimized MOs are subjected to the Boys localization procedure.[14] The calculated localized orbitals are very atomic in nature. The localized MOs for the transition state with C_{2v} symmetry in reaction 1 are plotted in Figure 1. (3) By using the localized MOs as a basis, a 20 × 20 CI is used to generate electronic structures and their

[⊗] Abstract published in *Advance ACS Abstracts,* January 1, 1997.

S1089-5639(96)01890-7 CCC: $14.00

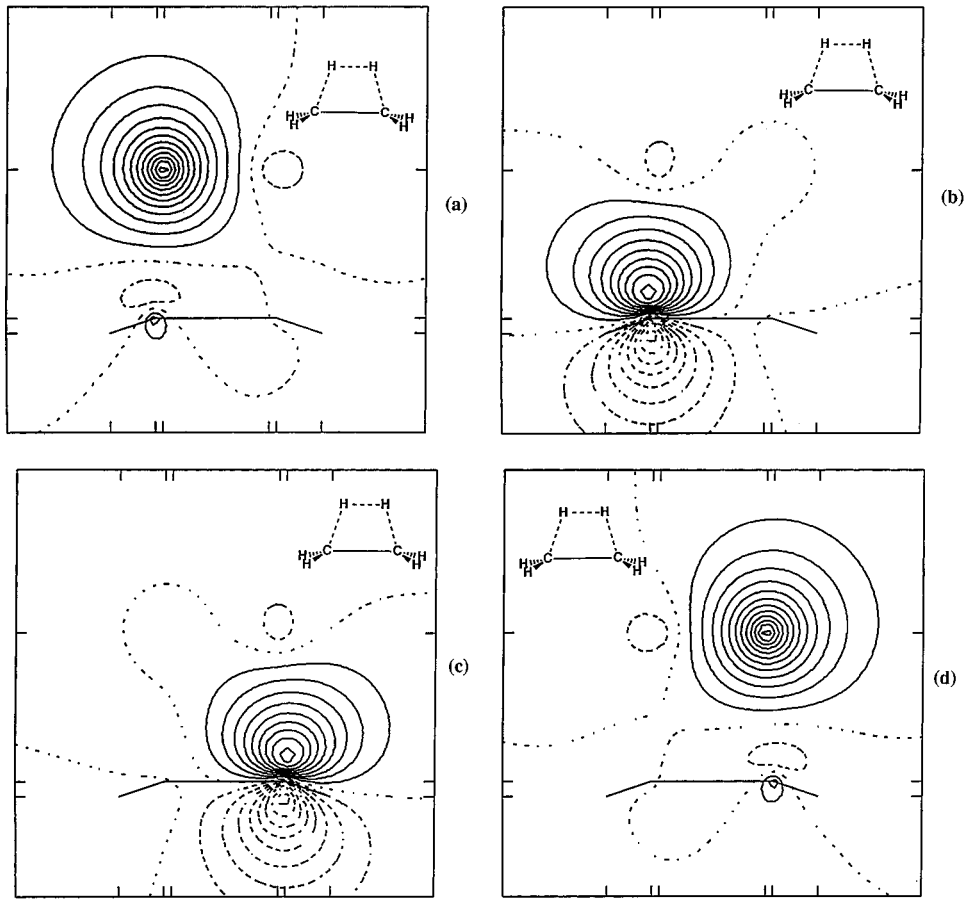

Figure 1. The localized CASSCF-optimized MOs for the transition state with C_{2v} symmetry for $H_2 + H_2C{=}CH_2$ reaction are plotted for (a) H (1s), (b) C ($2p_\pi$), (c) C ($2p_\pi$), and (d) H (1s).

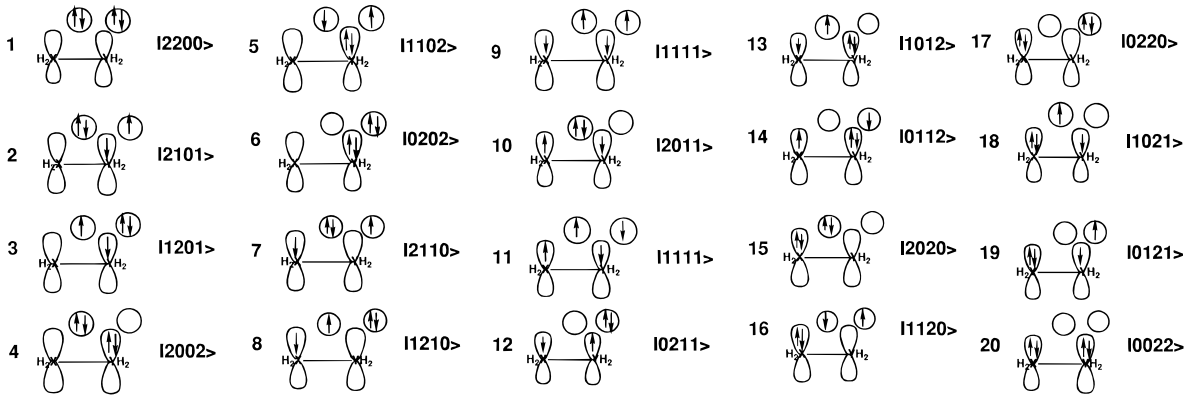

Figure 2. Electronic configurations from 20 × 20 CI.

relative weight in the ground state wave function. While a little tail remained in the obtained localized MOs as shown in Figure 1, we think that the main configurations can be used for the characterization of reaction. The 20 spin-adapted configurations generated are shown schematically in Figure 2.

The CI/LMO/CAS analysis calculations were performed with the GAMESS program.[15] The other calculations were carried out with the GAUSSIAN94 program.[16]

III. Results and Discussion

The structure shapes of stationary points for the treated reactions ($H_2X{=}YH_2 + H_2$: (X,Y) = (C,C), (Si,Si), (C,Si), (B,N), (B,P), (Al,N), and (Al,P)) are illustrated in Figure 3. Their geometry parameters are listed in Table 1. The total energies for their spaces and the relative energies are summarized in Tables 2 and 3, respectively.

A. $H_2X{=}XH_2 + H_2 \rightarrow H_3X{-}XH_3$ Reactions. First of all, 1,2-hydrogen addition into ethylene and disilene were treated. The least-motion paths for these reactions have C_{2v} symmetry, which are the symmetry forbidden reactions from the orbital symmetry rules. However the reaction paths with C_s or C_1 symmetry are the symmetry allowed reactions. The transition states (TS(C_{2v}) and TS(C_s)) with C_{2v} and C_s symmetries were calculated for the reactions $H_2 + H_2C{=}CH_2$ and $H_2Si{=}SiH_2$. For both systems of ethylene and disilene, each TS(C_{2v}) has two negative eigenvalues for their force constant matrix by the CAS/6-31G(d,p) calculation methods (CAS(4,4) and CAS(6,6)). The eigenvector of one negative eigenvalue corresponds to the reaction coordinate with a_1 symmetry for both systems. The other eigenvalue is 969 cm^{-1} (b_2 symmetry) for the ethylene system and 338 cm^{-1} (a_2 symmetry) for the disilene system by the CAS(6,6)/6-31G(d,p) method. Consequently their true

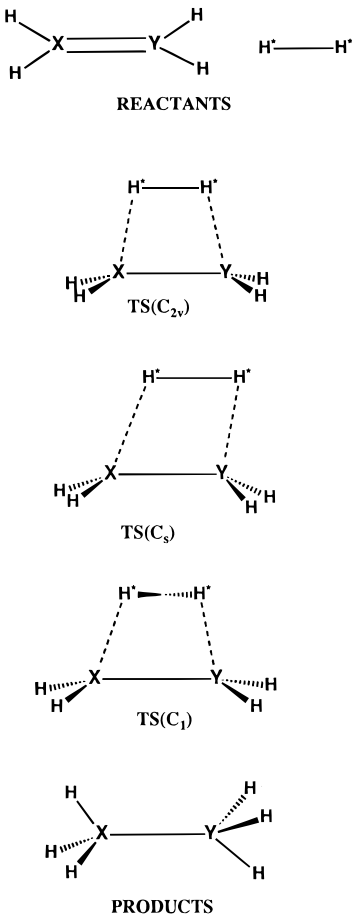

Figure 3. The structure shapes of stationary points.

transition states for the reactions of ethylene and disilene have C_s and C_1 symmetries, respectively. For the transition state of the disilene system with C_1 symmetry, the dihedral angle of H*−M−Si−Si (M: middle point of active hydrogen) is only 12° by the CAS(6,6) level.

For the reaction $H_2 + H_2C{=}CH_2$, the difference between the activation energy barriers at the transition states with C_{2v} and C_s symmetries is about 9 kcal/mol by the CAS(6,6) method and 17 kcal/mol by the MP2/CAS(6,6) methods. This energy difference for the ethylene system is only 8% by the CAS(6,6)/6-31G(d,p) calculation levels, and 17% by the MP2/CAS(6,6)/6-31G(d,p) levels. On the other hand, for the reaction $H_2 + H_2Si{=}SiH_2$, the difference between the energy barrier heights at the transition states with C_{2v} and C_s symmetries is 2.8 kcal/mol by the CAS(6,6)/6-31G(d,p) level and 13.2 kcal/mol by the MP2/CAS(6,6)/6-31G(d,p) levels. The energy difference is only 5% by the CAS(6,6)/6-31G(d,p) levels and 22% by the MP2/CAS(6,6)/6-31G(d,p) levels. At the transition states with C_s and C_1 symmetries for disilene system, the difference of the activation energy barriers is only 0.1 kcal/mol by the CAS(6,6) method. This small energy difference corresponds to the geometry difference at their transition states. As the results indicate, the reduced activation energies for the avoidance from the symmetry forbiddance ($C_{2v} \rightarrow C_s$ or C_1) are small (not drastic).

In order to electronically study mechanisms for the above two reaction pathways (C_{2v} and C_s), the reactions of the ethylene and disilene systems were analyzed along the IRC paths by the CI/LMO/CAS method. The relative weights of the electronic configurations at the points of the reactant side (RX = negative values), the transition state (RX = 0.0), and the product side (RX = positive values) for each system are summarized in

TABLE 1: Some Geometry Parameters of Stationary Points for the Treated Reactions by the CAS(6,6) and CAS(4,4) Methods[a]

stationary points					
X	Y	H*−H*[b]	X−Y	H*−X	H*−Y
			Reactant ($H_2X{=}YH_2 + H_2$)		
C	C	0.753	1.353 (1.338)		
Si	Si	0.753	2.236 (2.233)		
Si	C	0.753	1.740 (1.735)		
B	N	0.753	1.407 (1.389)		
B	P	0.753	1.883 (1.899)		
Al	N	0.753	1.790 (1.771)		
Al	P	0.753	2.337 (2.346)		
			TS(C_{2v} Symmetry)		
C	C	1.296 (1.268)	1.466 (1.448)	1.749 (1.743)	1.749 (1.743)
Si	Si	0.890 (0.903)	2.454 (2.408)	2.094 (2.548)	2.094 (2.548)
			TS(C_s Symmetry)		
C	C	1.458 (1.472)	1.490 (1.466)	1.489 (1.478)	1.700 (1.693)
Si	Si	0.968 (0.961)	2.425 (2.383)	1.699 (1.701)	2.006 (1.994)
Si	C	1.040 (1.059)	1.767 (1.747)	1.803 (1.838)	1.772 (1.810)
B	N	0.986 (1.004)	1.605 (1.574)	1.381 (1.363)	1.406 (1.409)
B	P	1.088 (1.133)	2.242 (2.104)	1.287 (1.278)	1.769 (1.783)
Al	N	0.994 (1.026)	1.941 (1.912)	1.414 (1.409)	1.826 (1.837)
Al	P	1.122 (1.111)	2.539 (2.538)	1.732 (1.728)	1.834 (1.838)
			TS(C_1 Symmetry)		
Si	Si	0.936 (0.950)	2.396 (2.375)	1.716 (1.682)	2.031 (1.973)
B	P	1.115	2.228	1.280	1.792
			Products ($H_3X{-}YH_3$)		
C	C		1.537	1.088	1.088
Si	Si		2.350	1.477	1.477
Si	C		1.891	1.477	1.088
B	N		1.689	1.202	1.014
B	P		1.982	1.198	1.396
Al	N		2.104	1.595	1.015
Al	P		2.587	1.589	1.397

[a] The values in parentheses were calculated by the CAS(4,4) method; units are angstroms. [b] H* means active hydrogen atom.

Tables 4−7. For the reaction of $H_2 + H_2C{=}CH_2$ with C_{2v} symmetry (Table 4), the weight of configuration 11 decreases from the reactant side to the product side and the weight of configuration 9 increases. That is to say, configuration 11 could be described as the interaction between singlet hydrogen and singlet ethylene coupled to give a singlet, and configuration 9 could be described as the interaction between triplet hydrogen and triplet ethylene coupled to give a singlet. From the results, this mechanism can be characterized by the transformation between the singlet and the triplet spin states for each π bond and H−H σ bond. Of course, the total spin state for the system is kept in the singlet state. We call this mechanism a *concerted reaction*. The variation in the weights of the configuration (Table 5) along the IRC path with C_s symmetry for $H_2 + H_2C{=}CH_2$ is similar to that for the reaction path with C_{2v} symmetry. Thus, both mechanisms on the C_{2v} and C_s paths are the *concerted reaction*. For the reaction of $H_2 + H_2Si{=}SiH_2$ with C_{2v} symmetry (Table 6), the weights of configuration 11 decreases from the reactant side to the product side and the weight of configuration 9 increases; it is the same pattern as that of $H_2 + H_2C{=}CH_2$. Accordingly, this mechanism is also the *concerted reaction*. For the reaction with C_s symmetry (Table 7), the weight of configuration 9 increases from the reactant side to the product side. On the other hand, the weight of configuration 11 does not change much such as those in the above reactions (the *concerted reaction*). The weight of configuration 16 decreases along the IRC path from the reactant side to the product side. Configuration 16 could be described by the polarization of the π bond. Consequently, we call this mechanism a *polarized* reaction. Thus, the reaction mechanisms

TABLE 2: Total Energies (hartree) for Various Species

methods	CAS(6,6)	MP2/CAS(6,6)	CAS(4,4)	MP2/CAS(4,4)	MP4/MP2
			Reactants		
H−H	−1.149 64	−1.161 77	−1.149 64	−1.161 77	−1.164 56
$H_2C{=}CH_2$	−78.093 27	−78.327 17	−78.067 34	−78.320 41	−78.353 79
$H_2Si{=}SiH_2$	−580.123 39	−580.300 71	−580.110 83	−580.294 76	−580.314 78
$H_2Si{=}CH_2$	−329.095 05	−329.305 43	−329.071 07	−329.294 42	−329.321 25
$H_2B{=}NH_2$	−81.541 34	−81.770 67	−81.513 58	−81.767 88	−81.796 89
$H_2B{=}PH_2$	−367.736 40	−367.946 49	−367.721 74	−367.934 03	−367.955 74
$H_2Al{=}NH_2$	−298.747 68	−298.962 34	−298.719 35	−298.958 90	−298.978 53
$H_2Al{=}PH_2$	−584.968 65	−585.152 76	−584.956 12	−565.145 87	−585.163 97
			Transition States		
H_2CHHCH_2 (C_{2v})	−79.068 30	−79.302 19	−79.046 28	−79.306 76	
H_2CHHCH_2 (C_s)	−79.082 78	−79.329 62	−79.058 56	−79.331 09	−79.374 37
$H_2SiHHSiH_2$ (C_{2v})	−581.186 40	−581.366 67	−581.173 36	−581.368 83	
$H_2SiHHSiH_2$(C_s)	−581.190 77	−581.387 82	−581.174 89	−581.389 25	−581.416 24
$H_2SiHHSiH_2$ (C_1)	−581.191 03	−581.387 80	−581.175 59	−581.395 81	−581.416 41
$H_2SiHHCH_2$ (C_s)	−330.150 44	−330.381 66	−330.127 25	−330.375 43	−330.406 73
H_2BHHNH_2 (C_s)	−82.599 71	−82.855 62	−82.572 64	−82.859 84	−82.892 84
H_2BHHPH_2 (C_s)	−368.832 23	−369.053 02	−368.826 38	−369.064 26	−369.090 62
H_2BHHPH_2 (C_1)	−368.833 56	−369.060 94			−369.092 11
$H_2AlHHNH_2$ (C_s)	−299.843 73	−300.082 51	−299.816 71	−300.081 80	−300.104 19
$H_2AlHHPH_2$ (C_s)	−586.055 83	−586.248 36	−586.044 03	−586.257 53	−586.276 29
			Products		
H_3C-CH_3					−79.584 12
$H_3Si-SiH_3$					−581.559 39
H_3Si-CH_3					−330.576 45
H_3B-NH_3					−82.961 72
H_3B-PH_3					−369.148 15
H_3Al-NH_3					−300.163 07
H_3Al-PH_3					−586.339 75

TABLE 3: Activation Energies and Heats of Reactions (ΔH) for H_2 + $H_2X{=}YH_2$ Reactions (kcal/mol)

		activation energy					
(X,Y)	sym	CAS (6,6)	MP2/CAS (6,6)	CAS (4,4)	MP2/CAS (4,4)	MP4/ MP2	ΔH MP4/MP2
(C,C)	C_{2v}	109.6	117.2	107.1	110.1		−41.3
	C_s	100.5	100.0	99.4	94.8	90.4	−41.4
(Si,Si)	C_{2v}	54.4	60.1	54.7	55.0		−50.2
	C_s	51.6	46.9	53.7	42.2	39.6	−50.2
	C_1	51.5	46.9	53.3	38.1	39.5	−50.2
(Si,C)	C_s	59.2	53.7	58.6	50.7	49.6	−56.9
(B,N)	C_s	57.3	48.2	56.8	43.8	43.0	−0.2
(B,P)	C_s	33.8	34.7	28.2	19.8	17.7	−17.5
	C_1	32.9	29.7				−17.5
(Al,N)	C_s	33.6	26.1	24.2	29.5	24.4	−12.5
(Al,P)	C_s	39.2	41.5	38.7	31.5	32.7	−7.0

on the C_s symmetry path for H_2 + $H_2Si{=}SiH_2$ are different from that on the C_{2v} symmetry path.

To study the reason for the difference of reaction mechanisms between ethylene and disilene systems with C_s symmetry, the triplet excitation, $\pi \rightarrow \pi^*$, energies and the π orbital polarization energies for ethylene and disilene were calculated by the MP4/6-31G(d,p)//MP2 level. For the triplet excitation energies, the three models with C_{2v}, C_s, and C_1 symmetries were calculated on the basis of the symmetry path from the above results. Namely the geometries of the models for the triplet state were optimized under the restriction of each symmetry (C_{2v}, C_s, and C_1). The triplet excitation energies were obtained from the energy difference between the ground state and the above model geometries. Accordingly, the obtained energies are adiabatic triplet excitation energies under the restriction of each symmetry (C_{2v}, C_s, and C_1). On the other hand, the calculations for the orbital polarization energies used the following model.

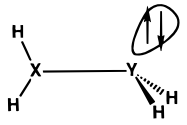

TABLE 4: CI Coefficients of LMO−CI Analyses along the IRC Path for H_2 + $H_2C{=}CH_2$ with C_{2v} Symmetry

no.	config	RX = −1.0	RX = −0.5	TS(0.0)	RX = 0.5	RX = 1.0
1	|2200>	−0.003	−0.011	−0.076	−0.133	−0.152
2	|2101>	−0.023	−0.050	−0.225	−0.326	−0.332
3	|1201>	−0.014	−0.023	−0.020	0.007	0.015
4	|2002>	0.162	0.138	−0.012	−0.150	−0.179
5	|1102>	0.274	0.265	0.176	0.051	0.036
6	|0202>	0.146	0.125	0.066	0.010	0.003
7	|2110>	0.014	0.023	0.020	−0.007	−0.015
8	|1210>	0.023	0.050	0.225	0.326	0.332
9	|1111>	0.012	0.050	0.412	0.598	0.571
10	|2011>	0.383	0.362	0.227	0.041	0.005
11	|1111>	0.677	0.716	0.671	0.396	0.342
12	|0211>	0.383	0.362	0.227	0.041	0.005
13	|1012>	0.026	0.054	0.215	0.306	0.333
14	|0112>	0.015	0.020	0.022	−0.001	−0.013
15	|2020>	0.146	0.125	0.066	0.010	0.003
16	|1120>	0.274	0.265	0.176	0.051	0.036
17	|0220>	0.162	0.138	−0.012	−0.150	−0.179
18	|1021>	−0.015	−0.020	−0.022	0.001	0.013
19	|0121>	−0.026	−0.054	−0.215	−0.306	−0.333
20	|0022>	−0.004	−0.012	−0.068	−0.119	−0.155

The model was assumed to have C_s symmetry, and the geometry was optimized. The orbital polarization energy was obtained from the energy difference between the ground state and the model geometries. These calculated energies are listed in Table 8. The absolute values of the calculated triplet excitation and the calculated orbital polarization energies cannot be compared directly because these models are very rough for both the transition state and each energy (triplet excitation and orbital polarization energies). However, we think these values can be used as a qualitative comparison for the classification of reaction mechanisms. From the above results by the CI/LMO/CAS analysis, the reactions for ethylene and disilene on the C_{2v} and C_s symmetry paths were classified into the concerted and polarized mechanisms. We assumed here that the transition state (energy barrier height) for the conserted mechanism relates to

TABLE 5: CI Coefficients of LMO−CI Analysis along the IRC Path for the H_2 + H_2C=CH_2 Reaction with C_s Symmetry

no.	config	RX = −1.0	RX = −0.5	TS(0.0)	RX = 0.5	RX = 1.0
1	|2200>	0.046	−0.077	−0.120	−0.140	−0.152
2	|2101>	−0.082	0.019	−0.110	−0.226	−0.286
3	|1201>	−0.134	0.157	0.166	0.135	0.093
4	|2002>	0.037	−0.002	−0.061	−0.075	−0.133
5	|1102>	0.136	−0.029	0.091	0.135	0.112
6	|0202>	0.133	−0.108	−0.072	−0.039	−0.016
7	|2110>	−0.303	0.339	0.287	0.152	0.064
8	|1210>	−0.200	0.234	0.292	0.323	0.329
9	|1111>	−0.372	0.511	0.589	0.586	0.559
10	|2011>	0.184	−0.059	0.056	0.084	0.056
11	|1111>	0.520	−0.383	−0.125	0.155	0.276
12	|0211>	0.311	−0.276	−0.237	−0.174	−0.105
13	|1012>	0.121	−0.047	0.091	0.222	0.299
14	|0112>	0.325	−0.372	−0.335	−0.232	−0.135
15	|2020>	0.129	−0.096	−0.061	−0.022	−0.004
16	|1120>	0.260	−0.248	−0.230	−0.141	−0.058
17	|0220>	0.124	−0.132	−0.169	−0.201	−0.206
18	|1021>	0.123	−0.135	−0.147	−0.108	−0.056
19	|0121>	0.168	−0.222	−0.317	−0.386	−0.386
20	|0022>	0.038	−0.065	−0.120	−0.168	−0.189

TABLE 6: CI Coefficients of LMO−CI Analysis along the IRC Path for the H_2 + H_2Si=SiH_2 Reaction with C_{2v} Symmetry

no.	config	RX = −0.5	TS(0.0)	RX = 0.5
1	|2200>	−0.039	−0.105	−0.190
2	|2101>	−0.138	−0.259	−0.373
3	|1201>	−0.107	−0.155	−0.114
4	|2002>	−0.027	−0.112	−0.173
5	|1102>	−0.011	−0.092	−0.090
6	|0202>	0.006	−0.018	−0.010
7	|2110>	0.107	0.155	0.114
8	|1210>	0.138	0.259	0.373
9	|1111>	0.091	0.247	0.487
10	|2011>	0.417	0.332	0.150
11	|1111>	0.743	0.643	0.416
12	|0211>	0.417	0.332	0.150
13	|1012>	0.090	0.153	0.233
14	|0112>	0.070	0.101	0.088
15	|2020>	0.006	−0.018	−0.010
16	|1120>	−0.011	−0.092	−0.090
17	|0220>	−0.027	−0.112	−0.173
18	|1021>	−0.070	−0.101	−0.088
19	|0121>	−0.090	−0.153	−0.233
20	|0022>	−0.011	−0.025	−0.063

the triplet excitation energies (the electron spin exchange from singlet to triplet) for each spaces (H_2 and H_2X=YH_2) and the transition state for the polarized mechanism relates to the orbital polarization energy on the basis of the model as shown in the above figure for each space.

From the assumed transition state models, reaction systems in Scheme 1 were also studied. For ethylene, the calculated triplet excitation energies for C_{2v} and C_s symmetries are almost the same (the difference: 3%). This fact corresponds to the small difference (9% by the CAS(6,6) method) in activation energies on the C_{2v} and C_s reaction paths. On the C_{2v} symmetry path, the activation energy of disilene is about 50% of that for ethylene. This can be explained from the triplet excitation energies of ethylene and disilene with C_{2v} symmetry. Namely, the triplet excitation energy of disilene with C_{2v} symmetry is about 54% of that of ethylene. Next, we would like to explain the mechanisms (concerted and polarized) for ethylene and disilene on the C_s symmetry paths. The calculated orbital polarization energy for ethylene is over 60% of the triplet excitation energy with C_s symmetry. On the other hand, the calculated orbital polarization energy for disilene is under 30%

TABLE 7: CI Coefficients of LMO−CI Analysis along the IRC Path for the H_2 + H_2Si=SiH_2 Reaction with C_s Symmetry

no.	config	RX = −0.5	TS(0.0)	RX = 0.5
1	|2200>	0.066	0.110	−0.207
2	|2101>	0.014	−0.098	0.264
3	|1201>	−0.055	0.046	−0.027
4	|2002>	−0.006	0.025	−0.105
5	|1102>	−0.006	−0.024	0.024
6	|0202>	0.018	0.006	0.000
7	|2110>	−0.256	0.296	−0.251
8	|1210>	−0.249	0.330	−0.444
9	|1111>	−0.204	−0.327	0.498
10	|2011>	−0.039	−0.154	0.166
11	|1111>	0.088	−0.077	0.261
12	|0211>	0.131	0.080	−0.018
13	|1012>	0.008	0.091	−0.221
14	|0112>	0.069	−0.046	0.017
15	|2020>	0.324	0.204	−0.052
16	|1120>	0.609	0.503	−0.228
17	|0220>	0.357	0.342	−0.237
18	|1021>	0.301	−0.296	0.146
19	|0121>	0.308	−0.342	0.281
20	|0022>	0.054	0.093	−0.104

TABLE 8: Triplet Excitation Energies and Orbital Polarization Energies for H_2X=YH_2 Molecule by MP4/6-31G(d,p)/MP2 Level (kcal/mol)

	triplet excitation			orbital polarization
	C_{2v}	C_s	C_1	
H_2C=CH_2	179.0	173.6	67.4	109.9
H_2Si=SiH_2	96.1	96.1	21.6	31.3
H_2Si=CH_2		42.4	36.0	57.2
H_2B=NH_2		123.9	107.9	32.7
H_2B=PH_2		82.0	65.2	10.6
H_2Al=NH_2		85.9	82.8	12.8
H_2Al=PH_2		60.0	58.6	3.6

SCHEME 1

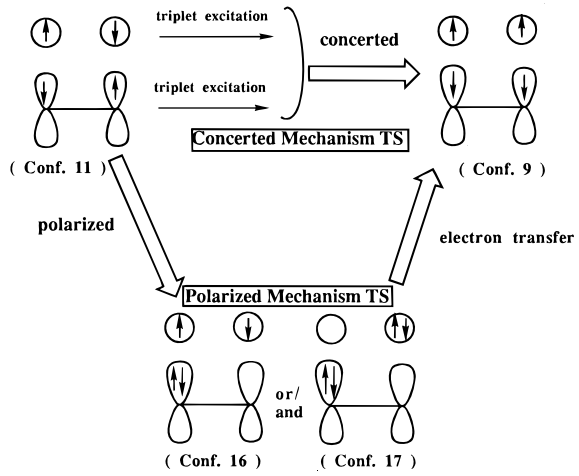

of the triplet excitation energy with C_s symmetry. Namely, the selection between the *concerted* mechanism or the *polarized* mechanism depends on whether the influence of the triplet excitation energy is dominant or whether the orbital polarization energy is dominant, and therefore selection between the mechanisms will somehow depend on the balance between these effects or perhaps by the ratio of one to the other. Hence, the reaction of the ethylene system occurs through the concerted mechanism for both C_{2v} and C_s symmetry paths. The reaction of the disilene system occurs through the concerted mechanism for the C_{2v} symmetry path and through the polarized mechanism for the C_s symmetry path. As this is stated here, it would seem that one could have the triplet excitation energy controlling the

TABLE 9: CI Coefficents of LMO−CI Analysis at the Transition States for $H_2 + H_2X{=}YH_2$ Reactions

no.	config	SiC (C_s)	BN (C_s)	BP (C_s)	AlN (C_s)	AlP (C_s)
1	|2200>	0.110	0.096	0.182	−0.100	0.158
2	|2101>	−0.007	0.112	0.224	0.096	0.177
3	|1201>	−0.141	−0.054	−0.008	−0.072	0.004
4	|2002>	−0.004	0.044	0.090	−0.030	0.064
5	|1102>	0.013	−0.046	−0.011	0.051	0.003
6	|0202>	0.068	0.011	−0.004	−0.022	−0.003
7	|2110>	−0.352	−0.189	0.351	0.179	−0.358
8	|1210>	−0.394	−0.337	0.380	0.370	−0.402
9	|1111>	−0.350	−0.425	0.370	−0.410	−0.340
10	|2011>	0.009	−0.115	0.223	−0.089	−0.218
11	|1111>	0.246	−0.152	0.209	−0.128	−0.227
12	|0211>	0.279	0.119	−0.010	0.176	−0.022
13	|1012>	0.022	−0.198	0.155	0.159	−0.129
14	|0112>	0.166	0.119	−0.003	−0.152	−0.019
15	|2020>	0.170	0.064	0.164	−0.051	0.154
16	|1120>	0.425	0.269	0.405	−0.261	0.429
17	|0220>	0.298	0.348	0.267	−0.383	0.309
18	|1021>	0.189	0.191	0.225	0.157	0.213
19	|0121>	0.243	0.495	0.261	0.493	0.256
20	|0022>	0.056	0.242	0.079	0.212	0.057

concerted mechanism while the orbital polarization energy is controlling the *polarized* mechanism.

B. $H_2X{=}YH_2 + H_2 \rightarrow H_3X{-}YH_3$. The reactions for five asymmetric systems ($H_2 + H_2X{=}YH_2$: X not equal to Y, (X,Y) = (Si,C), (B,N), (B,P), (Al,N), and (Al,P)) were treated. The transition states for these reactions have C_s symmetry, except for the (B,P) system by the CAS(6,6)/6-31G(d,p) method. These reactions were analyzed by the CI/LMO/CAS methods. The relative weights of the electronic configurations at the transition states for these systems are summarized in Table 9. The calculated results for these systems are similar to that of the disilene system with C_s symmetry. Namely, the weights of configurations 16 and 17 are large for all systems. The configurations 16 and 17 mean the polarization of the π bond of X=Y and the polarization of the π bond of X=Y and the σ bond of the active hydrogen, respectively. Thus, these reactions occur through the *polarized* mechanism.

Consider the relationship between the activation energy barrier heights for these systems and the triplet excitation or the orbital polarization energies for $H_2X{=}YH_2$ molecules. The activation energy barrier for the reaction $H_2Si{=}CH_2 + H_2$ is about 8 kcal/mol larger than that for the reaction $H_2Si{=}SiH_2 + H_2$ on the C_s pathway by the CAS(6,6)/6-31G(d,p) method. The calculated orbital polarization energy of $H_2Si{=}CH_2$ is about 26 kcal/mol larger than that of $H_2Si{=}SiH_2$. Hence the order relationship of the activation energies for both reactions corresponds with that of their calculated orbital polarization energies. On the other hand, the triplet excitation energy for $H_2Si{=}CH_2$ is about 54 kcal/mol less than that of $H_2Si{=}SiH_2$. This relationship is the opposite of that for their activation energies. That is to say, the reaction of the $H_2Si{=}CH_2$ system occurs through the *polarized mechanism* as shown in the results of the CI/LMO/CAS analysis. The activation energy barrier height for the reaction $H_2B{=}NH_2 + H_2$ is similar to those for the (Si,Si) and (Si,C) systems with C_s symmetry: the barrier height for the (B,N) system is in the middle of those for the (Si,Si) and (Si,C) systems. The orbital polarization energy of $H_2B{=}NH_2$ is also in the middle of those of the $H_2Si{=}SiH_2$ and $H_2Si{=}CH_2$ molecules. However the triplet excitation energy for $H_2B{=}NH_2$ is very large as compared with the triplet excitation energies for $H_2Si{=}SiH_2$ and $H_2Si{=}CH_2$. The reaction $H_2B{=}PH_2 + H_2$ does not lead to the product $H_3B{-}PH_3$; it leads to BH_3--H_3P weak complex as shown in a previous paper.[17] The activation energy barrier for the (Al,N) system is about 20 kcal/mol lower than those for the (Si,C) and (B,N) systems. The orbital polarization energy of the $H_2Al{=}NH_2$ molecule is also about 20 kcal/mol smaller than that of $H_2B{=}NH_2$. The activation energy barrier for the (Al,P) system is about 20 kcal/mol lower than those for the (Si,C) and (B,N) systems by the CAS(6,6) level. The orbital polarization energy of $H_2Al{=}PH_2$ is about 30 kcal/mol smaller than that of $H_2B{=}NH_2$. In comparison with the (Al,N) and (Al,P) systems, the order relationship of these activation energies does not correspond to that of their orbital polarization energies. In the reaction of the (Al,P) system, it is considered that the bond-breaking mechanism of the H_2 molecule becomes critical because of the small electron negativity of the phosphorus atom. Thus, the activation energy barrier heights for the above treated systems correlate closely with the orbital polarization energies of their π bonds. While the orbital polarization energy calculated here is a very rough approximation for the index of the *polarized* mechanisms, it is useful to estimate the qualitative reactivity.

Before concluding this section, we should note the relation between the reaction mechanisms (concerted and polarized) and the geometries of the transition states as shown in Table 1. For the reactions of ethylene and disilene, the transition states with C_{2v} symmetry are earlier than those with C_s symmetry because the H*−H* bond length for the C_{2v} symmetry transition states are longer than those for the C_s symmetry transition states. Similarly, this relation can be seen for the H*−X bond length in comparison with the transition states and the products. For the C_{2v} symmetry transition states, the H*−X bond length for the reactions of ethylene and disilene are 61% and 42% longer than those of the products, respectively. The H*−X bond length for the C_s symmetry transition states of ethylene and disilene are longer by 37% and 15% than those of the products, respectively. For other systems, the differences in the H*−X bond length between the transition states and their products are about under 22% ((Si,C) 22%, (B,N) 15%, (B,P) 7%, (Al,N) −11%, and (Al,P) 9%). From these facts, we suppose that the concerted transition state is earlier than the polarized transition state.

For the experimental energy barriers, we do not know the activation energies for the treated reactions. The energy barrier for $B_2H_6 + NH_3 \rightarrow H_2B{=}NH_2 + H_2 + BH_3$ was found to be 5.6 kcal/mol by infrared matrix isolation.[18] However, we have showed[19] that the reaction does not occur through the 1,2-hydrogen elimination mechanism.

IV. Conclusions

The reaction mechanisms of 1,2-hydrogen addition into π bonds of $H_2X{=}YH_2$ molecules were studied by ab initio MO methods. For X=Y systems (ethylene and disilene), there are two types of reaction pathways from the orbital symmetry rules. One is the least-motion pathway with C_{2v} symmetry, which is symmetry forbidden. The other is the reduced symmetry pathway with C_s or C_1 symmetry, which is symmetry allowed. For ethylene and disilene systems, the least-motion and the reduced symmetry pathways were calculated. The transition states on the least-motion pathways for both systems are not true transition states. The difference between the activation energy heights on the least-motion and on the reduced symmetry paths was 17% for ethylene system and 22% for disilene system in comparison with their activation energy heights on the least motion path by the MP2/CAS(6,6) level.

The CI/LMO/CAS analysis showed the following results. The reactions on the least-motion pathway for both ethylene and disilene systems occur through the *concerted* mechanism. While the reactions on the reduced symmetry paths (C_s or C_1 symmetry) for the ethylene system occur also through the

concerted mechanism, the reaction for disilene occurs through the *polarized* mechanism. The reactions for five asymmetric systems ($H + H_2X{=}YH_2$: (X,Y) = (Si,C), (B,N), (B,P), (Al,N), and (Al,P)) occur also through the *polarized* mechanism. These two types of reaction mechanisms were explained on the basis of the $\pi \rightarrow \pi^*$ triplet excitation energies and the π bond polarization energies for $H_2X{=}YH_2$ molecules. Therefore, 1,2-hydrogen addition into $H_2X{=}YH_2$ was classified into the *concerted* mechanism and *polarized* mechanism.

Acknowledgment. The present research is supported by a Grant-in-Aid for Scientific Research on Priority Area "Theory of Chemical Reactions" from the Ministry of Education, Science and Culture. The computer time was made available by the Computer Center of the Institute for Molecular Science and by the Information Systems Engineering Department of Osaka Sangyo University with its CONVEX C240 minisupercomputer.

References and Notes

(1) Woodward, R. B.; Hoffmann, R. *The Conservation of Orbital Symmetry*; Verlag Chemie: Weinheim, Germany, 1970.
(2) Gordon, M. S.; Truong, T. N.; Pople, J. A. *Chem. Phys. Lett.* **1986**, *130*, 245.
(3) Siria, J. C.; Duran, M.; Liedos, A.; Bertran, J. *J. Am. Chem. Soc.* **1987**, *109*, 7623.
(4) Gordon, M. S.; Truong, T. N.; Bonderson, E. K. *J. Am. Chem. Soc.* **1986**, *108*, 1425.
(5) Haviharan, P. C.; Pople, J. A. *Theor. Chim. Acta.* **1973**, *28*, 213. Gordon, M. S. *Chem. Phys. Lett.* **1980**, *76*, 163.
(6) Komornicki, A.; Ishida, K.; Morokuma, K.; Ditchfield, R.; Conrad, M. *Chem. Phys. Lett.* **1994**, *45*, 595.
(7) Roos, B. *In Advances in Chemical Physics*; Lawley, K. P., Ed.; Wiley: New York, 1987; Vol. 69, Part II, p 399.
(8) Pople, J. A.; Seeger, R.; Krishnan, R. *Int. J. Quantum Chem.* **1979**, *s11*, 149.
(9) Pople, J. A.; Binkley, J. S.; Seeger, R. *Int. J. Quantum Chem.* **1975**, *9*, 229. Pople, J. A.; Krishnan, R.; Schegel, H. B.; Binkley, J. S. *Int. J. Quantum Chem.* **1975**, *s13*, 225.
(10) McDouall, J. J.; Peasley, K.; Robb, M. A. *Chem. Phys. Lett.* **1988**, *148*, 183.
(11) Fukui, K. *J. Phys. Chem.* **1970**, *74*, 4161. Ishida, K.; Morokuma, K.; Komornicki, A. J. *Chem. Phys.* **1977**, *66*, 2153.
(12) Cundari, T. R.; Gordon, M. S. *J. Am. Chem. Soc.* **1991**, *113*, 5231.
(13) Sakai, S. submitted for publication.
(14) Foster, J. M.; Boys, S. F. *Rev. Mod. Phys.* **1960**, *32*, 296, 300.
(15) Schmidt, M. W.; Buldridge, K. K.; Boatz, J. A.; Jensen, J. H.; Koseki, S.; Gordon, M. S.; Nguyen, K. A.; Windus, T. L.; Elbert, S. T. *QCPE Bull.* **1990**, *10*, 52.
(16) Frisch, K. J.; Trucks, G. W.; Schlegel, H. B.; Gill, P. M. W.; Johnson, B. G.; Robb, M. A.; Cheseman, J. R.; Keith, T. A.; Petersson, G. A.; Montgomery, J. A.; Raghavachari, K.; Al-Laham, M. A.; Zakrzewski, V. G.; Ortiz, J. V.; Foresman, J. B.; Cislowski, J.; Stefanov, B. B.; Nanayakkara, A.; Challacombe, M.; Peng, C. Y.; Ayala, P. Y.; Chen, W.; Wong, M. W.; Andres, J. L.; Replogle, E. S.; Comperts, R.; Martin, R. L.; Fox, D. J.; Binkley, J. S.; DeFrees, D. J.; Baker, J.; Stewart, J. P.; Head-Gordon, M.; Gonzalez, C.; Pople, J. A., *GAUSSIAN94*; Gaussian, Inc.: Pittsburgh, PA, 1995.
(17) Sakai, S. *J. Phys. Chem.* **1995**, *99*, 9080.
(18) Carpenter, J. D.; Ault, B. S. *Chem. Phys. Lett.* **1992**, *197*, 171.
(19) Sakai, S. *J. Phys. Chem.* **1995**, *99*, 5883.